Thermodynamically consistent effective stress formulation for unsaturated soils across a wide range of soil saturation

Javad Ghorbani[1] · Jayantha Kodikara[1]

Abstract

We outline an extension of Biot's theory of dynamic wave propagation in fluid-saturated media, which can be used to model dynamic soil-structure interaction in frictionless conditions across a wide range of soil saturation levels. In this regard, we present a comprehensive analysis of experimental evidence, the thermodynamic, and the theoretical basis of using the degree of saturation as Bishop's parameter in unsaturated soils. The analysis highlights the limitations of using this parameter to accurately model unsaturated soil behaviour, particularly as the soil approaches dryness. Based on the analysis, a new definition of effective stress is proposed, and the associated work-conjugate pairs are identified. Recommendations are made for constitutive modelling using the new definition of effective stress. Finally, we introduce a fully coupled finite element contact model that utilises the new effective stress definition. Through numerical examples, we demonstrate the model's capability to control the vanishing capillary effect on soil-structure interaction as the soil dries.

1 Introduction

Biot's theory of dynamic wave propagation in fluid-saturated media [1, 2] is a seminal contribution to soil mechanics and has been widely used to predict the behaviour of saturated soils under dynamic loading conditions (e.g., in [3–6] and many more). The theory has been instrumental, particularly in offshore geomechanics. Nonetheless, in many instances, soils are in unsaturated states in nature and continuously interact with climate. Because air is in the pores, Biot's original theory cannot be used accurately.

To address this issue, researchers (e.g., [7, 8]) extended the theory to unsaturated states. The concept of Bishop's effective stress in unsaturated soil [9] was central in this extension, as it provides a smooth transition to Biot's theory for saturated media when the degree of saturation approaches unity. In the pioneering work on extension of Biot's theory to unsaturated soils [7, 8], the degree of saturation is chosen as Bishop's parameter. In [10], the author presented a theoretical basis

for such a choice based on an "averaging procedure". Also, thermodynamic bases for the use of the degree of saturation as Bishop's parameter were given in [11–13] among others.

However, the experimental evidence supporting this choice is mixed. More specifically, the use of the degree of saturation as Bishop's parameter has been called into question by several researchers, particularly when soils are close to the dry state [14–17]. Towards dryness, the contribution of capillary suction to the effective stress often disappears, an issue that can result in a loss of strength of the soil. Nonetheless, in many instances, the use of the degree of saturation as Bishop's parameter results in predicting an ever-increasing contribution of capillary near dryness and significant overestimation of the load capacity of soils. Additionally, some researchers (such as in [18, 19]) have shown that the degree of saturation may not even be a good approximation of the effective stress parameter near saturation.

To address the limitations of previous approaches, we conduct a comprehensive review of experimental evidence, thermodynamic principles, and theoretical models to evaluate the effectiveness of using the degree of saturation as the measure of effective stress. Based on our analysis, we propose a new definition for effective stress that improves accuracy over a wider range of saturation levels. Our equation accounts for the gradual decrease of capillary forces as

✉ Javad Ghorbani
  Javad.ghorbani@monash.edu

[1] ARC Smart Pavements Hub, Department of Civil
  Engineering, Monash University, Clayton, VIC 3108,
  Australia

saturation increases and can be adjusted to match the degree of saturation when necessary. Moreover, we focus on the implications of our proposed effective stress parameter for the constitutive modelling of unsaturated soils. With our proposed new definition of effective stress, we extend Biot's theory of dynamic wave propagation in fluid-saturated media to a wider range of saturation levels. Our approach involves developing a new computational framework for modelling frictionless dynamic soil-structure interaction across a broad range of saturation. This framework fully incorporates the effects of the new effective stress parameters, allowing us to gain greater control over simulating vanishing capillary effects on soil behaviour.

We begin by presenting the governing equations that describe the dynamics of unsaturated soils. Then, we introduce our new definition of effective stress and demonstrate how it improves accuracy across a wide range of saturation levels. Next, we identify work-conjugate pairs by analysing the internal energy of the unsaturated soil. This enables us to make recommendations for constitutive modelling based on these pairs. Finally, we present our fully coupled finite element contact model and demonstrate its capabilities through several numerical examples.

2 Dynamics of unsaturated soils

2.1 Conservation of mass

We consider a Representative Elementary Volume (REV) of unsaturated soil and define $\mathbf{u}_\alpha (\alpha = s, w, g)$ as displacement of the solid, water and gas in this domain. We also define the density of each phase by $\rho_\alpha (\alpha = s, w, g)$ as follows

$$\rho_\alpha = \frac{M^\alpha}{\Omega^\alpha} \tag{1}$$

where $M^\alpha (\alpha = s, w, g)$ is the mass of each phase and $\Omega^\alpha (\alpha = s, w, g)$ is the volume occupied by each phase with $\Omega = \sum_{(\alpha = s, w, g)} \Omega^\alpha$ represents the total volume of REV. Also, we define n^α as the fraction of the total volume occupied by each phase as follows:

$$n^\alpha = \frac{\Omega^\alpha}{\Omega} \tag{2}$$

where $\sum_{(\alpha = s, w, g)} n^\alpha = 1$. Also, the porosity of the soil n is defined by $n = n^w + n^g$. It is also useful to define partial density, ρ^α as follows:

$$\rho^\alpha = n^\alpha \rho_\alpha = \frac{M^\alpha}{\Omega} \tag{3}$$

The density of the mixture, ρ is defined by:

$$\rho = \sum_{(\alpha = s, w, g)} \rho^\alpha \tag{4}$$

Also, the degrees of saturation associated with water and gas are defined as follows:

$$S_\beta = \frac{n^\beta}{n} (\beta = w, g) \tag{5}$$

The conservation of mass can be written in the form of a differential equation, as follows:

$$\frac{\partial (\rho_\alpha n_\alpha)}{\partial t} + \text{div}(\rho_\alpha n_\alpha \dot{\mathbf{u}}_\alpha) = 0 \tag{6}$$

where div() denotes the divergence operator. By assuming $\dot{\mathbf{u}}_s = \dot{\mathbf{u}}$, we can write the conservation of mass of the solid as follows:

$$\frac{\partial ((1-n)\rho_s)}{\partial t} + \text{div}((1-n)\rho_s \dot{\mathbf{u}}) = 0 \tag{7}$$

Ignoring the spatial variation of the solid phase ($\text{grad}(\rho_s) = 0$, with grad representing the gradient operator), neglecting the compressibility of solid particles, and considering the concept of the material time derivative, $\frac{D(*)}{Dt} = \frac{\partial(*)}{\partial t} + \dot{\mathbf{u}}. \text{grad}(*)$ results in the following equation:

$$\frac{Dn}{Dt} = (1-n)\text{div}(\dot{\mathbf{u}}) \tag{8}$$

The velocity of the other phases, $\dot{\mathbf{u}}_\beta (\beta = w, g)$ can be written as:

$$\dot{\mathbf{u}}_\beta = \dot{\mathbf{u}} + \dot{\mathbf{u}}_{\beta s} \tag{9}$$

where $\dot{\mathbf{u}}_{\beta s}$ represents the velocity of water and gas relative to solid and is defined as follows:

$$\dot{\mathbf{u}}_{\beta s} = \frac{\dot{\mathbf{w}}^\beta}{n S_\beta} (\beta = w, g) \tag{10}$$

where $\dot{\mathbf{w}}^\beta$ represents the Darcy velocity.

Also, the conservation of mass for the fluid phases can be expanded as follows:

$$\frac{\partial (n S_\beta \rho_\beta)}{\partial t} + \text{div}(n S_\beta \rho_\beta \dot{\mathbf{u}}_\beta) = 0 \tag{11}$$

which can be expanded as follows:

$$S_\beta \rho_\beta \left(\frac{Dn}{Dt} \right) + n \rho_\beta \left(\frac{DS_\beta}{Dt} \right) + n S_\beta \left(\frac{D\rho_\beta}{Dt} \right)$$
$$+ n S_\beta \rho_\beta \text{div}(\dot{\mathbf{u}}) + \rho_\beta \text{div}(\dot{\mathbf{w}}^\beta) + \dot{\mathbf{w}}^\beta . \text{grad}(\rho_\beta) = 0 \tag{12}$$

In an isothermal environment, the rate of change in the fluid density is:

$$\frac{1}{\rho_\beta}\frac{D\rho_\beta}{Dt} = \frac{1}{K_\beta}\frac{Dp_\beta}{Dt}, \ (\beta = w, \ g) \tag{13}$$

where K_β is the bulk modulus of the fluid phases.

Using Eqs. (13) and (8) and the definition of the material derivative, we can write (12), after dividing it by ρ_β, as follows:

$$\frac{nS_\beta}{K_\beta}\frac{Dp_\beta}{Dt} + n\frac{DS_\beta}{Dt} + S_\beta \mathrm{div}(\dot{\mathbf{u}}) + \mathrm{div}(\dot{\mathbf{w}}^\beta)$$
$$+ \dot{\mathbf{w}}^\beta . \frac{1}{\rho_\beta}\mathrm{grad}(\rho_\beta) = 0 \tag{14}$$

2.2 Linear momentum balance

By defining $\boldsymbol{\sigma}^\alpha(\alpha = w, \ g, \ s)$, as the apparent stress tensor, the linear momentum balance for each phase in an arbitrary volume may be defined as follows:

$$\mathrm{div}(\boldsymbol{\sigma}^\alpha) + \rho^\alpha \mathbf{b} + \mathbf{I}^\alpha = \rho^\alpha \ddot{\mathbf{u}}_\alpha \tag{15}$$

where $\mathbf{b}$ is the gravitational acceleration and $\mathbf{I}^\alpha$ (where $\sum_{\alpha=w,\ g,\ s}\mathbf{I}^\alpha = 0$) represents the exchange of moments between phases due to the difference in the velocity of each phase [20]. Furthermore, the acceleration of water and air is defined by:

$$\ddot{\mathbf{u}}_\beta = \ddot{\mathbf{u}}_s + \ddot{\mathbf{u}}_{\beta s} + \mathrm{grad}\ (\dot{\mathbf{u}}_\beta).\dot{\mathbf{u}}_{\beta s}(\beta = w, \ g) \tag{16}$$

where $\ddot{\mathbf{u}}_s = \frac{\partial(\dot{\mathbf{u}})}{\partial t} + \mathrm{grad}(\dot{\mathbf{u}}).\dot{\mathbf{u}}$ and $\ddot{\mathbf{u}}_{\beta s} = \frac{\partial(\dot{\mathbf{u}}_{\beta s})}{\partial t} + \mathrm{grad}(\dot{\mathbf{u}}_{\beta s}).\dot{\mathbf{u}}$.

It should also be noted that we will consider $\ddot{\mathbf{u}} = \ddot{\mathbf{u}}_s$.

The linear momentum balance equation of the unsaturated soils can be obtained by the summation of all the individual momentum equations as follows:

$$\mathrm{div}(\boldsymbol{\sigma}) + \rho\mathbf{b} = \rho\ddot{\mathbf{u}} + \left[\rho^g\ddot{\mathbf{u}}_{ws} + \rho^w\ddot{\mathbf{u}}_{gs}\right] \tag{17}$$

2.3 Balance of energy

The rate of change in the internal energy of the unsaturated soil E_I is defined as follows:

$$\frac{DE_I}{Dt} = \mathcal{P} - \frac{DE_k}{Dt} \tag{18}$$

where E_k is the kinetic energy and $\mathcal{P}$ is the total power. We can write the kinetic energy as follows:

$$\frac{DE_k}{Dt} = \sum_{\alpha=w,\ g,\ s}\int_\Omega \rho^\alpha\ddot{\mathbf{u}}_\alpha.\dot{\mathbf{u}}_\alpha d\Omega \tag{19}$$

Also, by defining surface tractions $\mathbf{t}^\alpha$ as follows $\mathbf{t}^\alpha = \boldsymbol{\sigma}^\alpha.\mathbf{n}^*$ we get:

$$\mathcal{P} = \sum_{\alpha=w,\ g,\ s}\int_\Gamma \mathbf{t}^\alpha.\dot{\mathbf{u}}_\alpha d\Gamma + \int_\Omega (\rho^\alpha\mathbf{b} + \mathbf{I}^\alpha).\dot{\mathbf{u}}_\alpha d\Omega \tag{20}$$

Using the Gaussian theorem, we can rewrite Eq. (20) as follows:

$$\mathcal{P} = \sum_{\alpha=w,\ g,\ s}\int_\Omega \left(\mathrm{div}(\boldsymbol{\sigma}^\alpha.\dot{\mathbf{u}}_\alpha) + (\rho^\alpha\mathbf{b} + \mathbf{I}^\alpha).\dot{\mathbf{u}}_\alpha\right)d\Omega \tag{21}$$

where $\mathrm{div}(\boldsymbol{\sigma}^\alpha.\dot{\mathbf{u}}_\alpha) = \boldsymbol{\sigma}^\alpha : \mathrm{grad}(\dot{\mathbf{u}}_\alpha) + \mathrm{div}(\boldsymbol{\sigma}^\alpha).\dot{\mathbf{u}}_\alpha$.

2.3.1 Effective stress

In unsaturated states, the concept of effective stress can be represented by the equation proposed by Bishop, which takes the form:

$$\boldsymbol{\sigma}' = \boldsymbol{\sigma} + \chi p_w\mathbf{I} + (1 - \chi)p_g\mathbf{I} \tag{22}$$

where χ is the effective stress or Bishop's parameter and is bounded between 0 and 1 in the limits of dryness and saturation, respectively. Also, $\mathbf{I}$ represents the identity tensor.

It is important to note that stress components are assumed to be positive in tension, while pore air and water pressure are assumed to be positive in compression. Also, negative strain denotes compression. Following this sign convention, we can write:

$$\boldsymbol{\sigma}' = \boldsymbol{\sigma}_{net} - \chi p_c\mathbf{I} \tag{23}$$

where $p_c = p_g - p_w$ represents matric suction and $\boldsymbol{\sigma}_{net} = \boldsymbol{\sigma} + p_g\mathbf{I}$ represents the net stress. Moreover, the term χp_c regulates the contribution of capillary water to effective stress and is sometimes referred to as "suction stress", a term that, to the best of the authors' knowledge, was proposed originally in [21–23] and adopted later in other studies such as [24, 25].

Despite the general agreement that the effective stress parameter (χ) is influenced by soil properties, formulating a universally accepted definition of effective stress for unsaturated soils continues to be a challenge due to the difficulties inherent in direct measurement of this quantity in laboratory conditions. To address this challenge, various approaches have been employed to determine this parameter, resulting
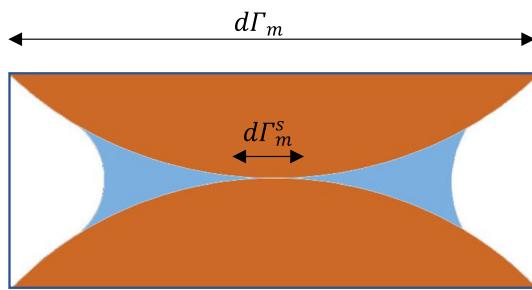
Fig. 1 A schematic representation of a cut surface of unsaturated soils on a sufficiently small scale where menisci can be observed

in several proposed definitions, each with specific predictive capabilities (e.g., [10, 17, 26, 27] and others). One early proposal is the use of the degree of saturation as the effective stress parameter which has been widely used in the literature (e.g., in [6, 28–31] and many more).

As noted in [13], in order to describe the behaviour of unsaturated porous media, two general strategies are commonly used: macro-mechanics and micro-mechanics. The former includes phenomenological approaches, while the latter includes averaging theories. While the degree of saturation has been proposed as an effective stress parameter from a phenomenological standpoint, there is only mixed experimental support for its use (e.g., [19, 32]). It is also illuminating to explore the underlying assumptions behind the volume averaging method that was used to derive the degree of saturation as the effective stress.

In an idealised sketch of a cut surface of unsaturated soils on a sufficiently small scale where menisci can be observed, the presence of water, gas, and solid particles is shown in Fig. 1. If the total force exerted on the surface is sustained only by water, air, and solid particles, we may write:

$$\boldsymbol{\sigma}_m d\Gamma_m = \boldsymbol{\sigma}_{m-s} d\Gamma_m^s + \boldsymbol{\sigma}_{m-w} d\Gamma_m^w + \boldsymbol{\sigma}_{m-g} d\Gamma_m^g \tag{24}$$

where $\boldsymbol{\sigma}_m$, $\boldsymbol{\sigma}_{m-s}$, $\boldsymbol{\sigma}_{m-w}$, and $\boldsymbol{\sigma}_{m-g}$ are the stresses sustained by the total mixture, of solid particles, water, and gas in this scale whereas $d\Gamma_m$, $d\Gamma_m^s$, $d\Gamma_m^w$, and $d\Gamma_m^g$ are the total contact surface and the contact surfaces occupied by each phase. It should be noted that our analysis assumes that material properties and thermodynamic quantities at the interface with other constituents may exhibit step discontinuities. As pointed out in [33] the "contractile skin" or the interface between air and water may exhibit different behaviour from the air and solid phase and thus have a separate contribution to the stress components. This contribution is ignored in our analysis similar to [11, 12, 20].

If an area or surface fraction in this scale is defined by:

$$A_m^\alpha = \frac{d\Gamma_m^\alpha}{d\Gamma_m} \tag{25}$$

we may write:

$$\boldsymbol{\sigma}_m = \boldsymbol{\sigma}_{m-s} A_m^s + \boldsymbol{\sigma}_{m-w} A_m^w + \boldsymbol{\sigma}_{m-g} A_m^g \tag{26}$$

The area fractions in Eq. (26) must be transformed into commonly measured soil properties at a macro scale. This transformation can be achieved through the scaling procedure outlined in [20, 34]. However, the resulting transformation of Eq. (26) will involve area fractions at a macro scale with limited practical application and no straightforward measurement technique. To connect these quantities to volume fractions at a macro scale (which are quantities that are commonly measured in geotechnical tests), researchers in [10] made an assumption based on Delesse's principle. According to Delesse's law, the volume fractions on a smaller scale $n_m^\alpha = \frac{d\Omega_m}{d\Omega}$ are equal to the area fractions A_m^α in an isotropic mixture on each cut surface. Therefore, [10] assumed

$$\boldsymbol{\sigma}_m = \boldsymbol{\sigma}_{m-s} n_m^s + \boldsymbol{\sigma}_{m-w} n_m^w + \boldsymbol{\sigma}_{m-g} n_m^g \tag{27}$$

The average stress tensor, $\boldsymbol{\sigma}$ at a macroscale is then obtained in [20] as follows:

$$\boldsymbol{\sigma} = \frac{1}{\Omega} \sum_{\alpha=s, w, g} \int_{\Omega^\alpha} \boldsymbol{\sigma}_{m\_\alpha} d\Omega_m = \sum_{\alpha=s, w, g} n^\alpha \boldsymbol{\sigma}_\alpha \tag{28}$$

where $\boldsymbol{\sigma}_\alpha$ is the "intrinsic phase-averaged" stress tensor of each phase. It is also possible to rewrite Eq. (28) as follows:

$$\boldsymbol{\sigma} = (1-n)\Big(\boldsymbol{\sigma}_s - S_w \boldsymbol{\sigma}_w - S_g \boldsymbol{\sigma}_g\Big) + S_w \boldsymbol{\sigma}_w + S_g \boldsymbol{\sigma}_g \tag{29}$$

by assuming shear terms are negligible in non-solid stress tensors, we can define:

$$\boldsymbol{\sigma}_\beta = -\mathbf{I} p_\beta (\beta = w, g) \tag{30}$$

Using (30) in (29) and rearrangement of (29) yields:

$$(1-n)\Big(\boldsymbol{\sigma}_s - S_w \boldsymbol{\sigma}_w - S_g \boldsymbol{\sigma}_g\Big) = \boldsymbol{\sigma} + S_w p_w \mathbf{I} + S_g p_g \mathbf{I} \tag{31}$$

By comparing (31) and (22), it may be deduced that $\boldsymbol{\sigma}' = (1-n)\Big(\boldsymbol{\sigma}_s - S_w \boldsymbol{\sigma}_w - S_g \boldsymbol{\sigma}_g\Big)$ and Bishop's parameter is equal to the degree of saturation, thereby, the relationship between effective stress and total stress is written as follows

$$\boldsymbol{\sigma} = \boldsymbol{\sigma}' - S_w p_w \mathbf{I} - S_g p_g \mathbf{I} \tag{32}$$

It is noteworthy that the averaging approach described above does not differentiate between capillary water and adsorbed water (which relatively has a negligible effect on the soil strength) and assumes an equal contribution of these

two forms of water to effective stress. However, this assumption can be inconsistent with observations in soils close to the dry state (e.g., [24]). Particularly in granular soils, a significant loss of strength may occur as the soil becomes dry due to the loss of capillary water and the resulting decrease of effective stress. As the soil desaturates from the saturated state, the product of $S_w p_c$ initially increases and the contribution of the term $S_w p_c$ in effective stress is expected to reach a peak. After this stage, further drying will result in a decline in the contribution of $S_w p_c$ as noted in [15, 24], among others. Failure to capture the decrease in effective stress arising from the loss of capillary pressure can result in a significant overestimation of the soil strength and predicting very stiff and unrealistic behaviour toward dryness. It is important to note that there can be exceptions. For instance, in slurry clays, $S_w p_c$ may not exhibit an apparent reduction as they near dryness. The behaviour of these soils near dryness is characterised by a more decisive role of micropores, which limit water mobility. As these soils approach dryness, micropores can significantly shrink and it becomes exceedingly difficult for capillary breakage to occur. Consequently, the decrease in $S_w p_c$ may not be visible. However, for the usual compacted soils where macropores are more influential, the contribution of suction to the effective stress is generally expected to diminish.

In [16], the authors highlighted the limitations of some commonly used Soil Water Retention Curves (SWRC) in capturing such a peak in $S_w p_c$. For instance, if the equation developed in [35] which indicates $S_w = \begin{cases} \left(\frac{p_c}{P_b}\right)^{-\lambda_b} & for \ p_c > P_b \\ 1 & for \ p_c \le P_b \end{cases}$, (with P_b as the air-entry value and λ_b as a fitting parameter), is selected, the resulting $S_w p_c$ for $p_c > P_b$ will be $P_b^{-\lambda_b}(p_c)^{1-\lambda_b}$, an ever-increasing function of suction when $\lambda_b < 1$. Also, for the so-called van Genuchten model [36] shown in Eq. (33) (with m_v and n_v as two fitting parameters) by taking the first derivative of χp_c it can be shown that the function will only yield a peak when $m_v n_v > 1$.

$$S_w = \left(1 + \left(\frac{p_c}{P_b}\right)^{n_v}\right)^{-m_v} \tag{33}$$

The preceding discussion may suggest that the main factor behind this anomaly is the selection of the mathematical model employed to fit the water retention data. However, as pointed out in [16], there are instances in experimental data where the SWRC model is accurately fitted, yet the resulting effective stress values are implausible.

The generalisation of the discussed averaging method to account for various forms of water in soil pores is a complex task, as it can potentially introduce averaged quantities

observed at very small scales into the equation for effective stress which can be arduous to measure, particularly in unsaturated soils. In this regard, we can resort to phenomenological methods such as an effective degree of saturation proposed in [16]. In this study, the authors introduced the "microstructural water ratio", ξ_m to develop a new definition for effective stress which appears to be more suitable for cohesive soils and is as follows:

$$\chi = \frac{S_w - \xi_m}{1 - \xi_m} \tag{34}$$

A similar expression is also given in [14] where the authors assumed that below a residual degree of saturation, all water in soil pores exists in the form of adsorbed water and does not contribute to effective stress. The equation uses a residual degree of saturation, S_{w_res} as follows:

$$\chi = \frac{S_w - S_{w\_res}}{1 - S_{w\_res}} \tag{35}$$

However, both definitions are unable to adequately model χ in the transitional range toward dryness where capillary water is gradually disappearing. In other words, both models predict that the term χp_c vanish abruptly near the dry state, while experimental evidence suggests that there is a gradual decline in effective stress toward dryness [16] although, as stated earlier, there can be exceptions such as slurry clays subjected to drying, which may not show such a decline. A more comprehensive equation for χ that can simulate such a gradual decline in capillary effect is proposed in [17] as follows

$$\chi = \frac{S_w - \xi_m}{1 - \xi_m} + \frac{1}{n_a}\ln\left(1 + \exp\left(-n_{smoth}\frac{S_w - \xi_m}{1 - \xi_m}\right)\right) \tag{36}$$

where the term $\frac{1}{n_a}\ln\left(1 + \exp\left(-n_{smoth}\frac{S_w - \xi_m}{1 - \xi_m}\right)\right)$ (with n_a and n_{smooth} as two material parameters) ensures a smooth decrease in the effective stress parameter toward dryness. Nonetheless, the function appears to be strictly applicable to cohesive soils in which water that is stored in "microstructures" can potentially influence effective stress. Even when it is assumed that $\xi_m \to 0$ (e.g., for modelling granular soils), the proposed equation will yield $\chi > 0$ when $S_w \to 0$. However, this may seem inconsistent with the understanding that at $S_w = 0$, the influence of water should completely diminish, removing any suction-imposed influence on Bishop's effective stress. Although in this situation other forces (of a different nature) might be present in the soil pores, capturing the effect of such forces on the soil stiffness generally falls outside the realm of Bishop's effective stress. It also appears that $\chi > 1$ for the case of saturation unless it is bounded by an additional constraint. An additional difficulty may arise from the experimental determination of ξ_m.
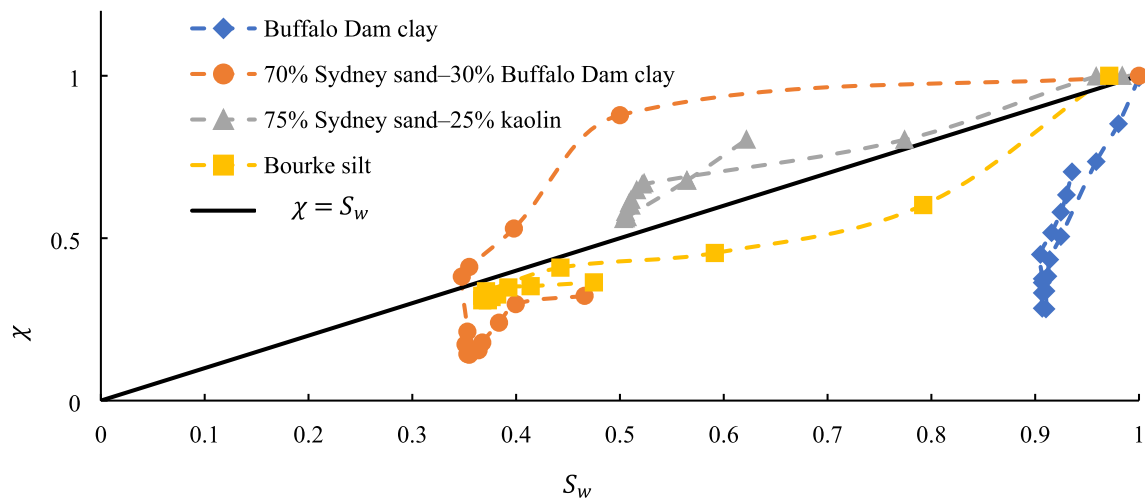
Fig. 2 The relationship between the degree of saturation and effective stress, data from [18]

Despite their limitations, an important aspect of the equations proposed in [17] and [14] is that they assume that the relationship between χ and S_w is independent of hydraulic hysteresis. This assumed characteristic has an important advantage when it comes to calibrating the effective stress parameters. A recent study in [19] also argued that the relationship between χ and S_w can be considered to be independent of hydraulic hysteresis with reasonable accuracy. This assumption is adopted in this study because of simplification although there is only mixed and limited experimental support for this assumption. For instance, Fig. 2 demonstrates the results reported in [18] on the relationship between χ and S_w in four types of soils subjected to shearing to the critical state in drying and wetting paths. The results indicate that in most cases the relationship between the degree of saturation and effective stress can be assumed independent of hysteresis with reasonable accuracy. Also, the degree of saturation can serve as a reasonable approximation of the effective stress parameter χ for "Sydney Sand" with 25% fines, particularly in near saturation and up to a moderate degree of saturation. Therefore, a refined version of χ should have the ability to converge to the degree of saturation when necessary.

The identified limitations of the effective stress parameter, extracted from the volume averaging technique, necessitate a pragmatic solution for refining the contributions from pore water and air pressure. To facilitate this, we introduced a correction factor, α_{eff} to the degree of saturation, with the intention of improving the predicted form of effective stress from the volume averaging technique and providing more precise control over the contribution of capillary water to the effective stress. Importantly, the assumption is that incorporating the correction term, α_{eff}, will scale n^w and n^g in

Eq. (29) to their enhanced equivalents, n_{eff}^w and n_{eff}^g, respectively, yielding the following equation:

$$\boldsymbol{\sigma} = (1 - n)\boldsymbol{\sigma}_s + n_{eff}^w\boldsymbol{\sigma}_w + n_{eff}^g\boldsymbol{\sigma}_g \tag{37}$$

where $n_{eff}^w = n\alpha_{ff}S_w$. This equation in combination with the one above, leads to the derivation of n_{eff}^g, which should satisfy the ensuing conditions:

$$n_{eff}^w + n_{eff}^g = n \tag{38}$$

This requirement implies that

$$n_{eff}^g = n(1 - \alpha_{ff}S_w) \tag{39}$$

By defining $\chi = \alpha_{ff}S_w$, we aim to take into account the following conditions that are outlined per the earlier discussions:

(1) The product of $\alpha_{eff} \cdot S_w$ should smoothly approach one at saturation and zero at dryness.
(2) α_{eff} should be capable of explaining the gradual decline of effective stress toward dryness, and its decline should be controlled by adjustable parameters.
(3) The parameters of α_{eff} should be readily obtainable from the macroscopic behaviour of soils.
(4) α_{eff} should not be affected by hydraulic hysteresis.
(5) α_{eff} should have the ability to converge to unity when needed, this allows recovery of the degree of saturation as Bishop's parameter.

A function that can satisfy these conditions is as follows:

$$\alpha_{eff}(S_w) = S_w^{\left(\frac{\beta_1}{S_w^{\beta_2}}\right)-1} \tag{40}$$

which yields the following form for the effective stress parameter:

$$\chi = S_w^{\left(\frac{\beta_1}{S_w^{\beta_2}}\right)} \tag{41}$$

where β_1 and β_2 are two material parameters controlling the effective stress parameters.

Figure 3.a demonstrates that as β_2 approaches zero and β_1 remains at one, the effective stress parameter converges towards the degree of saturation. When β_2 is decreased, the effective stress parameter decreases at a slower rate. In Fig. 3.b, it can be observed that when β_1 is less than one, the values of the effective stress parameter can initially exceed the degree of saturation. As β_1 increases within this range, the deviation of χ from S_w decreases. When $\beta_1 > 1$, an increase in β_1 causes the effective stress parameter to decrease more rapidly.

Figure 4 also illustrates the model's ability to reproduce the data collected in [18], as it effectively captures the effective stress over a wide range of saturation degrees and soil types using only two parameters. The pairs of $[\beta_1, \beta_2]$ are respectively set to [0.003,6.0], [0.75,0.02], [1.35,0.01], and [9.0,1.0] for "70% Sydney sand- 30% Buffalo Dam clay", "75% Sydney sand- 30% Buffalo Dam clay", "Bourke silt", and "Buffalo Dam clay" in these simulations.

2.3.2 Work-conjugate pairs

Based on (18) and after some manipulations we obtain:

$$\frac{DE_I}{Dt} = \int_\Omega \boldsymbol{\sigma} : \text{grad}(\dot{\mathbf{u}})d\Omega + \sum_{\beta=w,g} \int_\Omega \boldsymbol{\sigma}^\beta : \text{grad}(\dot{\mathbf{u}}_{\beta s})d\Omega \tag{42}$$

and the rate of internal energy per unit volume, e_I will be as follows:

$$\frac{De_I}{Dt} = \boldsymbol{\sigma} : \text{grad}(\dot{\mathbf{u}}) + \sum_{\beta=w,g} \boldsymbol{\sigma}^\beta : \text{grad}(\dot{\mathbf{u}}_{\beta s}) \tag{43}$$

Based on the proposed definition of effective stress parameter, we can write:

$$\boldsymbol{\sigma}^w = -n\alpha_{eff}S_w p_w \mathbf{I} \tag{44}$$

and

$$\boldsymbol{\sigma}^g = -n(1 - \alpha_{eff}S_w)p_g\mathbf{I} \tag{45}$$

where per Eq. (10), (44) and (45), we can obtain:

$$\boldsymbol{\sigma}^w : \text{grad}(\dot{\mathbf{u}}_{ws}) = -n\alpha_{eff}S_w p_w \text{div}\left(\frac{\dot{\mathbf{w}}^w}{nS_w}\right) \tag{46}$$

and

$$\boldsymbol{\sigma}^g : \text{grad}(\dot{\mathbf{u}}_{gs}) = -n(1 - \alpha_{eff}S_w)p_g\text{div}\left(\frac{\dot{\mathbf{w}}^g}{nS_g}\right) \tag{47}$$

Also, we can write:

$$\text{div}\left(\frac{\dot{\mathbf{w}}^\beta}{nS_\beta}\right) = \dot{\mathbf{w}}^\beta.\text{grad}\left(\frac{1}{nS_\beta}\right) + \frac{1}{nS_\beta}\text{div}(\dot{\mathbf{w}}^\beta) \tag{48}$$

where the definition of $\text{div}(\dot{\mathbf{w}}^\beta)$ from Eq. (14)yields:

$$\text{div}\left(\frac{\dot{\mathbf{w}}^\beta}{nS_\beta}\right)$$
$$= -\frac{1}{nS_\beta}\left(\frac{nS_\beta}{K_\beta}\frac{Dp_\beta}{Dt} + n\dot{S}_\beta + S_\beta\text{div}(\dot{\mathbf{u}}) + \frac{\dot{\mathbf{w}}^\beta}{\rho_\beta}.\text{grad}(\rho_\beta)\right)$$
$$+ \dot{\mathbf{w}}^\beta.\text{grad}\left(\frac{1}{nS_\beta}\right) \tag{49}$$

Since $\text{grad}(\rho_\beta) = \text{grad}\left(\frac{\rho^\beta}{nS_\beta}\right)$, we get:

$$\text{grad}(\rho_\beta) = \rho^\beta\text{grad}\left(\frac{1}{nS_\beta}\right) + \frac{1}{nS_\beta}\text{grad}(\rho^\beta) \tag{50}$$

Using (50) in (49)gives:

$$\text{div}\left(\frac{\dot{\mathbf{w}}^\beta}{nS_\beta}\right)$$
$$= -\frac{1}{nS_\beta}\left(\frac{nS_\beta}{K_\beta}\frac{Dp_\beta}{Dt} + n\dot{S}_\beta + S_\beta\text{div}(\dot{\mathbf{u}}) + \frac{\dot{\mathbf{w}}^\beta}{\rho^\beta}.\text{grad}(\rho^\beta)\right) \tag{51}$$

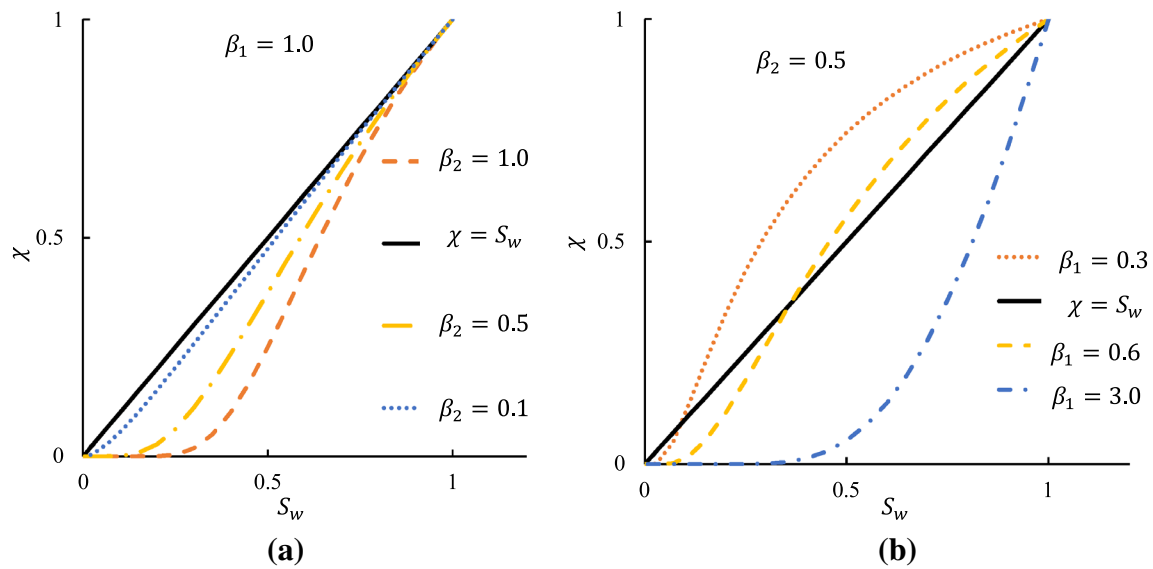By substituting (51) in (46) and (47), and using the result in (43), we obtain:

$$\frac{De_I}{Dt} = \boldsymbol{\sigma}' : \text{grad}(\dot{\mathbf{u}}) + \sum_{\beta=w,g} n\alpha_{eff}^\beta p_\beta\dot{S}_\beta + R \tag{52}$$

where we also define:

$$\alpha_{eff}^w = \alpha_{eff}, \quad \alpha_{eff}^g = \left(\frac{1 - \alpha_{eff}S_w}{S_g}\right),$$
$$and \quad \alpha_{eff}^{gw} = \alpha_{eff}^g - \alpha_{eff}^w \tag{53}$$
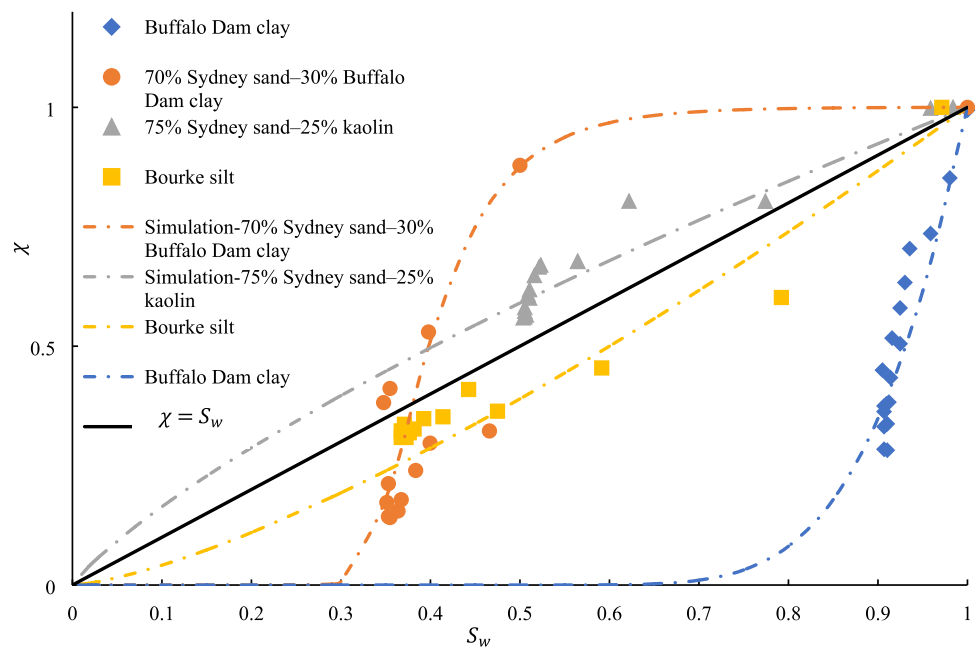
and

$$R = \sum_{\beta=w,g} = p_\beta\left(\frac{n\alpha_{eff}^\beta S_\beta}{K_\beta}\frac{Dp_\beta}{Dt} + \alpha_{eff}^\beta\frac{\dot{\mathbf{w}}^\beta}{\rho^\beta}.\text{grad}(\rho^\beta)\right) \tag{54}$$

Fig. 3 The influence of β_1 and β_2 on the relationship between the degree of saturation and effective stress

Fig. 4 Model predictions of the data reported in [18]

where $\frac{n\alpha_{eff}^{\beta} S_{\beta}}{K_{\beta}} \frac{Dp_{\beta}}{Dt}$ represents the effect of the compressibility of water and gas in the internal energy term and the convective term $\alpha_{eff}^{\beta} \frac{\dot{\mathbf{w}}^{\beta}}{\rho^{\beta}}.\mathrm{grad}(\rho^{\beta})$ is associated with the internal energy arising from the relative flow and generally serves as the thermodynamic basis for the constitutive models for fluid flow [37, 38].

Equations (52) to (54) indicate that obtaining a complete picture of the internal energy in unsaturated soil mixtures requires taking into account not only the energy contribution effective stress but also other terms involving the rate of changes in the degree of saturation, water pressure, air

pressure and spatial variations of partial density of water and gas.

Considering all these aspects in constitutive modelling of unsaturated soils is not practically possible. Therefore, a compromise between theoretical rigour and practicality must be made. This involves identifying the terms that have the most significant impact on the model while sacrificing some degree of theoretical complexity. As stated earlier, this analysis assumes incompressible solid particles, and we further assume that the internal energy term associated with the compressibility of water is also negligible. Recalling Eq. (13),

$\frac{1}{\rho_g}\frac{D\rho_g}{Dt} = \frac{1}{K_g}\frac{Dp_g}{Dt}$, we can revise Eq. (54) as follows:

$$R = p_g n \alpha_{eff}^g S_g \frac{1}{\rho_g}\frac{D\rho_g}{Dt} + p_w \alpha_{eff}^w \frac{\dot{\mathbf{w}}^w}{\rho^w}.\text{grad}\left(\rho^w\right)$$
$$+ p_g \alpha_{eff}^g \frac{\dot{\mathbf{w}}^g}{\rho^g}.\text{grad}(\rho^g) \tag{55}$$

where the first term may be viewed as the unit power of scaled partial air pressure, $n\alpha_{eff}^g S_g p_g$, in compressing the air volume (under a condition where the air mass is conserved). The terms associated with the spatial variations of ρ^w and ρ^g may also be assumed to be negligible, leading to the following simplified version of the internal energy rate per unit volume:

$$\frac{De_I}{Dt} = \boldsymbol{\sigma}' : \text{grad}(\dot{\mathbf{u}}) - n\alpha_{eff}^w p_c \dot{S}_w$$
$$- n\alpha_{eff}^{gw} p_g \dot{S}_w + p_g n \alpha_{eff}^g S_g \frac{1}{\rho_g}\frac{D\rho_g}{Dt} \tag{56}$$

Equation (56) can be compared to those derived in [11] and [12]. These authors used the degree of saturation as the effective stress parameter, and if we apply the discussed simplifying assumptions to their derivations of the internal energy rate per unit volume, they obtained:

$$\frac{De_I}{Dt} = \boldsymbol{\sigma}'' : \text{grad}(\dot{\mathbf{u}}) - np_c \dot{S}_w + p_g n S_g \frac{1}{\rho_g}\frac{D\rho_g}{Dt} \tag{57}$$

where $\boldsymbol{\sigma}''$ is the effective stress tensor when assuming χ approaches S_w. If $\alpha_{eff} \rightarrow 1$, we will obtain $\alpha_{eff}^{gw} \rightarrow 0$ and $\alpha_{eff}^w \rightarrow 1$ and $\alpha_{eff}^g \rightarrow 1$, $\chi \rightarrow S_w$, and $\boldsymbol{\sigma}' \rightarrow \boldsymbol{\sigma}''$. In such a condition, the equation derived in this work and those derived in [11] and [12] will be identical. Thus, their equations may be regarded as a special case of the presented formulations when $\alpha_{eff} \rightarrow 1$.

The energy Eq. (56) can be simplified by neglecting terms associated with air pressure, which are usually much smaller than those related to suction and effective stress. As α_{eff}^{gw} approaches zero near saturation, the energy term related to the change in the degree of saturation paired with $n\alpha_{eff}^{gw} p_g$ will be negligible. Although this term is not generally zero near dryness, the small slope of SWRC makes any change in the degree of saturation negligible. Additionally, due to the small contribution of pore air pressure (which can be in the form of free air close to dryness), the associated work can also be assumed negligible. Notably, as α_{eff}^w approaches zero close to dryness, the term $n\alpha_{eff}^w p_c \dot{S}_w$ will also approach zero. These simplifying assumptions lead to the conclusion that, similar to Biot's theory for fluid-saturated porous media, the internal energy of the soil is primarily influenced by Terzaghi's effective stress in saturation. However, the internal energy experiences a transitional range where the energy terms associated with suction and effective stress in unsaturated states are dominant. Finally, as the soil dries and the contribution of capillary pressure diminishes, the energy term associated with suction gradually vanishes, leaving only the energy contribution from net stress. Therefore, we write the simplified energy term as follows:

$$\frac{De_I}{Dt} = \boldsymbol{\sigma}' : \text{grad}(\dot{\mathbf{u}}) - n\alpha_{eff}^w p_c \dot{S}_w \tag{58}$$

which indicates the presence of an additional stress-like quantity $n\alpha_{eff}^w p_c$ that is paired with the degree of saturation in the energy term.

The free energy density per an arbitrary unit volume of the mixture, denoted by e_f, can be defined as $e_f = e_I - TS$ where S is the total entropy density per unit volume of the mixture, and $T > 0$ is the absolute temperature. In the absence of heat exchange and source, the Clausius–Duhem inequality implies that $\frac{DS}{Dt} \geq 0$. Since T is positive, we can also write:

$$T\frac{DS}{Dt} = \frac{De_I}{Dt} - \frac{De_f}{Dt} \geq 0 \tag{59}$$

Using $\frac{De_I}{Dt}$ per Eq. (58) gives:

$$\boldsymbol{\sigma}' : \dot{\boldsymbol{\varepsilon}} - n\alpha_{eff}^w p_c \dot{S}_w - \frac{De_f}{Dt} \geq 0 \tag{60}$$

where $\boldsymbol{\varepsilon}$ is the strain tensor that is assumed to be defined $\boldsymbol{\varepsilon} = \boldsymbol{\varepsilon}_e + \boldsymbol{\varepsilon}_p$ (with $\boldsymbol{\varepsilon}_e$ and $\boldsymbol{\varepsilon}_p$ as elastic and plastic strain tensors respectively). We assume that the changes in the degree of saturation is a result of the changes in suction and volumetric strain (e.g., [39, 40]). This assumption allows the expansion of Eq. (60) as follows:

$$\overline{\overline{\boldsymbol{\sigma}}}' : \dot{\boldsymbol{\varepsilon}} - n\bar{p}_c \dot{\tilde{p}}_c - \frac{De_f}{Dt} \geq 0 \tag{61}$$

where $\overline{\overline{\boldsymbol{\sigma}}}' = \left(\boldsymbol{\sigma}_{net} - \alpha_{eff}(S_w)\left(S_w + e\frac{\partial S_w}{\partial e}\right)p_c\mathbf{I}\right)$ with e being the void ratio and $\overline{p}_c = \alpha_{eff}^w p_c$ is an effective suction. The dimensionless and strain-like quantity attributed to suction is denoted as $\dot{\tilde{p}}_c$ where $\dot{\tilde{p}}_c = \frac{\partial S_w}{\partial p_c}\dot{p}_c$. Similarly, we assume that $\dot{\tilde{p}}_c$ can be decomposed into plastic and elastic parts as follows, $\tilde{p}_c = \tilde{p}_{c_e} + \tilde{p}_{c_p}$ with subscripts e and p denoting elastic and plastic components, respectively.

We can define the free energy of the mixture as a function of the elastic strain, the dimensionless and strain-like quantity associated with suction, and a vector of internal plastic variables, and a vector of internal plastic variables, $\mathbf{q}_I$ as follows:

$$e_f = e_f\left(\boldsymbol{\varepsilon}_e, \tilde{p}_{c_e}, \mathbf{q}_I\right) \tag{62}$$

which yields:

$$\frac{De_f}{Dt} = \frac{\partial e_f}{\partial \boldsymbol{\varepsilon}_e} : \dot{\boldsymbol{\varepsilon}}_e + \frac{\partial e_f}{\partial \tilde{p}_{c_e}} \dot{\tilde{p}}_{c_e} + \frac{\partial e_f}{\partial \mathbf{q}_I} : \dot{\mathbf{q}}_I \tag{63}$$

Using (63), we can write (61) as follows:

$$\left(\overline{\overline{\boldsymbol{\sigma}}}' - \frac{\partial e_f}{\partial \boldsymbol{\varepsilon}_e} \right) : \dot{\boldsymbol{\varepsilon}}_e - n \left(\bar{p}_c - \frac{\partial e_f}{\partial \tilde{p}_{c_e}} \right) \dot{\tilde{p}}_{c_e} + \overline{\overline{\boldsymbol{\sigma}}}'$$
$$: \dot{\boldsymbol{\varepsilon}}_p - n \bar{p}_c \tilde{p}_{c_p} - \frac{\partial e_f}{\partial \mathbf{q}_I} : \dot{\mathbf{q}}_I \geq 0 \tag{64}$$

where it may be concluded that the term $\frac{\partial e_f}{\partial \boldsymbol{\varepsilon}_e}$ indicates a constitutive equation above relates $\overline{\overline{\boldsymbol{\sigma}}}'$ and the solid matrix elastic strain tensor $\boldsymbol{\varepsilon}_e$. Also, by defining $\mathbf{A}_q = -\frac{\partial e_f}{\partial \mathbf{q}_I}$, we get the reduced dissipation inequality as follows:

$$\overline{\overline{\boldsymbol{\sigma}}}' : \dot{\boldsymbol{\varepsilon}}_p - n \bar{p}_c \dot{\tilde{p}}_{c_p} + \mathbf{A}_q : \dot{\mathbf{q}}_I \geq 0 \tag{65}$$

If we assume a convex and smooth yield surface, $F\left(\overline{\overline{\boldsymbol{\sigma}}}', \overline{p}_c, \dot{\mathbf{q}}_I \right) \leq 0$ for satisfying the above inequality, the principle of maximum dissipation indicates that:

$$\dot{\boldsymbol{\varepsilon}}_p = \dot{\lambda} \frac{\partial F}{\partial \overline{\overline{\boldsymbol{\sigma}}}'}, \ \dot{\tilde{p}}_{c_p} = \dot{\lambda} \frac{\partial F}{\partial \overline{p}_c}, \ \text{and } \dot{\mathbf{q}}_I = \dot{\lambda} \frac{\partial F}{\partial \dot{\mathbf{q}}_I} \tag{66}$$

where $\dot{\lambda}$ is a non-negative quantity that also satisfies the condition of $\dot{\lambda} F = 0$.

It is important to note that our assumptions and their consequent results in Eqs. (63) to (66) suggest that a describing a complete picture of the behaviour of unsaturated soil mixture may require the consideration of the terms associated with $\overline{p}_c$ and $\overline{\overline{\boldsymbol{\sigma}}}'$ (even in the elasticity range) with a possible incremental relationship of the following form:

$$\begin{pmatrix} \dot{\overline{\overline{\boldsymbol{\sigma}}}}' \\ \dot{\bar{p}}_c \end{pmatrix} = \begin{pmatrix} \mathbf{D}_{\overline{\overline{\sigma}}\overline{\overline{\sigma}}} & \mathbf{D}_{\overline{\overline{\sigma}}\bar{p}_c} \\ \mathbf{D}_{\bar{p}_c\overline{\overline{\sigma}}} & D_{\bar{p}_c\bar{p}_c} \end{pmatrix} \begin{pmatrix} \dot{\boldsymbol{\varepsilon}} \\ \dot{\tilde{p}}_c \end{pmatrix} \tag{67}$$

where $\mathbf{D}_{\overline{\overline{\sigma}}\overline{\overline{\sigma}}}$ indicates elastoplastic stress–strain matrix, $D_{\overline{p}_c\overline{p}_c}$ describes the incremental relationship between $\tilde{p}_{c_p}$ and $\overline{p}_c$ whereas the other two are coupling matrices in this incremental relationship. The incremental form of $\overline{\overline{\boldsymbol{\sigma}}}'$ (for the particular case of $\alpha_{eff}(S_w) = 1$) was highlighted in [41] and more recently in [42]. It may also be noted that since the effect of porosity in the term $n\dot{\bar{p}}_c$ can also be captured by the constitutive matrices, $\dot{\bar{p}}_c$ may be used in place of $n\dot{\bar{p}}_c$ as shown in Eq. (67).

It is important to note that the above constitutive modelling approach is only one possible approach, and there may be many other alternatives that can be defined and used. For instance, we may define an elastic and plastic portion of the degree of saturation (S_{w_e} and $\dot{S}_{w_p}$, respectively) and express the degree of saturation rate as the sum of these two components, i.e., $\dot{S}_w = \dot{S}_{w_e} + \dot{S}_{w_p}$. In this case, we can define free energy as follows:

$$e_f = e_f\left(\boldsymbol{\varepsilon}_e, S_{w_e}, \mathbf{q}_I \right) \tag{68}$$

which leads to the following dissipation inequality:

$$\boldsymbol{\sigma}' : \dot{\boldsymbol{\varepsilon}}_p - n\overline{p}_c \dot{S}_{w_p} + \mathbf{A}_q : \dot{\mathbf{q}}_I \geq 0 \tag{69}$$

and the following incremental relationship:

$$\begin{pmatrix} \dot{\boldsymbol{\sigma}}' \\ \dot{\bar{p}}_c \end{pmatrix} = \begin{pmatrix} \mathbf{D}_{\boldsymbol{\sigma}\boldsymbol{\sigma}} & \mathbf{D}_{\boldsymbol{\sigma}\overline{p}_c} \\ \mathbf{D}_{\overline{p}_c\boldsymbol{\sigma}} & D_{\overline{p}_c\bar{p}_c} \end{pmatrix} \begin{pmatrix} \dot{\boldsymbol{\varepsilon}} \\ \dot{S}_w \end{pmatrix} \tag{70}$$

Where $\mathbf{D}_{\boldsymbol{\sigma}\boldsymbol{\sigma}}$ has a role similar to $\mathbf{D}_{\overline{\overline{\sigma}\sigma}}$ but describes the incremental relationship between strain and $\boldsymbol{\sigma}'$ instead of $\overline{\overline{\boldsymbol{\sigma}}}'$. It is important to emphasise that the above assumption implies that even in the elastic range, the rate of change in the degree of saturation still contributes to the behaviour of the unsaturated soil mixture. This version of effective stress appears to be more prevalent in the constitutive modelling of unsaturated soils. For the particular case of $\alpha_{eff} = 1$, the effective stress tensor coincides with those adopted in [29, 40, 43–47] and many more. Also, the presented assumptions on decomposing the degree of saturation into reversible and irreversible parts and using the degree of saturation as the effective stress parameter appear to be adopted in studies such as [30, 48, 49] and more recently in [50].

Another possibility is the use of net stress as follows:

$$\begin{pmatrix} \dot{\boldsymbol{\sigma}}_{net} \\ \dot{\bar{p}}_c' \end{pmatrix} = \begin{pmatrix} \mathbf{D}_{\boldsymbol{\sigma}_{net}\boldsymbol{\sigma}_{net}} & \mathbf{D}_{\boldsymbol{\sigma}_{net}\overline{p}_c'} \\ \mathbf{D}_{\bar{p}_c'\boldsymbol{\sigma}_{net}} & D_{\bar{p}_c'\bar{p}_c'} \end{pmatrix} \begin{pmatrix} \dot{\boldsymbol{\varepsilon}} \\ \dot{e}_w \end{pmatrix} \tag{71}$$

where $\overline{p}_c' = \frac{\overline{p}_c}{1+e}$ and $e_w = S_w.e$. Similarly, $\mathbf{D}_{\boldsymbol{\sigma}_{net}\boldsymbol{\sigma}_{net}}$ describes the incremental relationship between net stress and strain and the other matrices have a similar role to their counterparts in the previous cases. For the particular case of $\chi = S_w$, in [51] and [52], the authors were among those who mentioned this possibility.

While the theoretical frameworks presented above show promise, enforcing the numerous constraints they require is difficult in practice due to experimental limitations. For instance, the associated flow rule assumption is usually inadequate for describing granular soil behaviour and overconsolidated clays (e.g., [53]). Furthermore, many elasticity equations are phenomenological models and hypoelastic, with the sole constraint that strain is incrementally recovered upon unloading. However, these models can violate general thermodynamic restrictions in an isolated system (e.g., [54, 55]). Additionally, obtaining precise experimental measurements of the required elasticity matrices can be a significant

challenge. For many practical applications, the elastic range is only described by using $\mathbf{D}_{\sigma\sigma}$ (or its counterparts in other arrangements) as an incremental relationship only between the chosen stress tensor and strain. These elasticity models are typically generalisations of existing elastic matrices for saturated soils by substituting Terzaghi's effective stress with unsaturated effective stress. If this assumption is followed, the internal energy term associated with the degree of saturation may only be considered in the dissipation inequality (an assumption that appears to be used in [12, 56]) and as a term that will have negligible contribution in the elasticity range. This assumption relaxes some of the above constraints and can lead to the development of a simpler constitutive equation for unsaturated soils. In this context, to describe the behaviour of unsaturated soils using the proposed effective stress definition we may use the following incremental relationship:

$$\begin{pmatrix} \dot{\boldsymbol{\sigma}}' \\ \dot{\bar{p}}_c \end{pmatrix} = \begin{pmatrix} \mathbf{D}_{\sigma\sigma} & \mathbf{D}_{\sigma\bar{p}_c} \\ \mathbf{D}_{\bar{p}_c\sigma} & D_{\bar{p}_c\bar{p}_c} \end{pmatrix} \begin{pmatrix} \dot{\boldsymbol{\varepsilon}} \\ \dot{S}_w \end{pmatrix} \tag{72}$$

Referring to the arrangement discussed in Eqs. (61) to (67), it is worth mentioning an alternative phenomenological approach that can avoid the difficulties associated with obtaining the incremental term $\alpha_{eff}(S_w)\left(S_w + e\frac{\partial S_w}{\partial e}\right)$ in the definition of $\overline{\overline{\boldsymbol{\sigma}}}'$. For a particular case where $\alpha_{eff}(S_w) = 1$, [41] showed that a phenomenological function B (which takes only suction as input) can be defined in such a manner that

$$B(p_c) = \left(S_w + e\frac{\partial S_w}{\partial e}\right) \tag{73}$$

However, if $B(p_c)$ is explicitly given using effective stress data, Eq. (73) adds a new constraint where the evolution of the degree of saturation with respect to void ratio must be obtained from B. Further discussions on this approach can be found in [57].

The above suggestions serve as general guidelines for selecting appropriate work-conjugate pairs when an alternative to the degree of saturation is chosen as the effective stress parameter. We would like to also emphasise the potential usefulness of $\overline{p}_c$ as a stress-like quantity that can be incorporated to develop hardening laws that are valid over a broader range of saturation, especially near dryness. This quantity vanishes at the limits of saturation and dryness and, when combined with appropriate hardening law, can facilitate modelling the gradual loss of strength toward the dry state.

Finally, it is worth noting that the idea of pinpointing a comprehensive effective stress definition that, when

utilised in isolation in constitutive models, can unravel various aspects of soil behaviour such as collapse and shear, can be appealing. However, deriving such a definition and establishing a thermodynamics basis for it can be an exceedingly challenging task. As a result, following our previous discussions, a more pragmatic approach may be more viable. This involves the synthesis of a phenomenological definition of effective stress with an additional constitutive modelling quantity, such as $\overline{p}_c$, to shed light on various aspects of unsaturated soil behaviour.

Still, the necessity for an additional stress-like component does not necessarily imply its universal application in all aspects of the constitutive model's formulations. Instead, there are worthwhile practical simplification strategies to consider. One such strategy acknowledges the fundamental role of the critical state in traditional soil plasticity. It is based on the widely accepted assumption that the internal friction angle remains relatively constant across different saturation levels, even under fully saturated conditions (e.g., [30] and many others). This approach makes it possible to determine the χ parameter through shear data analysis. In this context, χ would be a parameter that when adjusted will result in a unique internal friction angle covering a wide range of saturation levels.

Moreover, the incorporation of an additional constitutive modelling variable such as $\overline{p}_c$ can effectively handle other facets of soil behaviour, such as isotropic hardening, which often correlates with isotropic compression data [58]. This proposition presents itself as one potential systematic framework for the constitutive modelling of unsaturated soils.

3 Finite element simulations

Here we present a finite element discretisation of the dynamics of unsaturated soils that can also model frictionless contact with impervious solids as outlined in [59]. Similar to [60], this approach takes displacement, suction, and pore water pressure as primary unknown variables, although alternative arrangement can also be done e.g., by taking displacement, pore water pressure and pore air pressure [61].

The finite element equations can be obtained based on the weak forms of Eqs. (17) and (14). It is worth recalling some of the key simplifying assumptions before presenting the weak forms. They include ignoring the compressibility of solid particles, an isothermal and chemically reactive environment, and ignoring the spatial variations of solid density. In addition to these, following [20], we assume $\ddot{\mathbf{u}}_{\beta s}$ is negligible.

Considering $\delta p_g = \delta p_c + \delta p_w$, Eq. (17) can lead to the following weak form:

$$\int_\Omega \delta p_w \left(A_w\right) d\Omega + \int_\Omega \left(\delta p_c + \delta p_w\right)\left(A_g\right) d\Omega$$
$$+ \int_{\Gamma_{qw}} \delta p_w \left[\dot{\mathbf{w}}^w . \mathbf{n}^* - \overline{w}^w\right] d\Gamma$$
$$- \int_{\Gamma_{qg}} \left(\delta p_c + \delta p_w\right)\left[\dot{\mathbf{w}}^g . \mathbf{n}^* - \overline{w}^g\right] d\Gamma = 0 \tag{74}$$

where

$$A_\beta = \frac{n S_\beta}{K_\beta} \frac{D p_\beta}{Dt} + n \frac{D S_\beta}{Dt} + S_\beta \text{div}\,(\dot{\mathbf{u}})$$
$$+ \text{div}\left(\dot{\mathbf{w}}^\beta\right) + \dot{\mathbf{w}}^\beta . \frac{1}{\rho_\beta} \text{grad}(\rho_\beta) \tag{75}$$

In addition to the presented conservation of mass and linear momentum balance of the mixture, we assume a generalised Darcy's law, which can be defined in the following form [7]:

$$\dot{\mathbf{w}}^\beta = \mathbf{k}_\beta\left[-\text{grad}(p_\beta) + \rho_\beta(\mathbf{b} - \ddot{\mathbf{u}})\right], \ (\beta = w, g) \tag{76}$$

where that $\mathbf{k}_w$ and $\mathbf{k}_g$ are the permeability matrices of the medium governing the flow of the pore fluids, defined by

$$\mathbf{k}_\beta = \mathbf{k}_{int} \cdot \frac{k_{r\beta}}{\eta_\beta} \tag{77}$$

The relative permeability of the water and air phases, k_{rw} and k_{rg}, respectively, are defined as the ratio between the permeability at an unsaturated state and when fully saturated for which we have used the van Genuchten model. Thus, k_{rw} and k_{rg} are bounded between 0 and 1. The intrinsic or absolute permeability matrix of the soil is denoted by $\mathbf{k}_{int}$ and the viscosity of each fluid is denoted by η_β.

Furthermore, Eq. (14) leads to the following weak form:

$$\int_\Omega \delta u \left(\mathbf{L}^T \boldsymbol{\sigma} + \rho \mathbf{b} - \rho \ddot{\mathbf{u}}\right) d\Omega + \int_{\Gamma_t} \delta u \left(\bar{\mathbf{t}} - \mathbf{I}_\sigma^T \boldsymbol{\sigma}\right) d\Gamma = 0 \tag{78}$$

The imposed Dirichlet boundary conditions for the primary variables on the boundaries are:

$$\mathbf{u} = \bar{\mathbf{u}} \text{ on } \Gamma_u \tag{79}$$

$$p_w = \overline{p}_w \text{ on } \Gamma_{p_w} \tag{80}$$

$$p_w = \overline{p}_c \text{ on } \Gamma_{p_c} \tag{81}$$

whereas the Neumann boundary conditions on the prescribed tractions and fluxes are:

$$\mathbf{I}_\sigma^T \boldsymbol{\sigma} = \bar{\mathbf{t}} \text{ on } \Gamma_t \tag{82}$$

$$\mathbf{k}_w\left[-\text{grad}(p_w) + \rho_w(\mathbf{b} - \ddot{\mathbf{u}})\right].\mathbf{n}^* = \overline{w}_w \text{ on } \Gamma_{q_w} \tag{83}$$

$$\mathbf{k}_g\left[-\text{grad}(p_g) + \rho_g(\mathbf{b} - \ddot{\mathbf{u}})\right].\mathbf{n}^* = \overline{w}_g \text{ on } \Gamma_{q_g} \tag{84}$$

where $\overline{w}_\beta$ ($\beta = w, g$) are the prescribed values of the outflow rate of non-solid phase on the permeable boundaries Γ_{q_β} ($\beta = w, g$).

In addition, we define,

$$\mathbf{I}_\sigma^T = \begin{bmatrix} n_x & 0 & 0 & n_y & 0 & n_z \\ 0 & n_y & 0 & n_x & n_z & 0 \\ 0 & 0 & n_z & 0 & n_y & n_x \end{bmatrix} \tag{85}$$

and

$$\mathbf{n}^* = \begin{bmatrix} n_x \\ n_y \\ n_z \end{bmatrix} \tag{86}$$

with $n_\alpha (\alpha = x, y, z)$ as a unit outward normal vector to the boundaries in x, y and z directions.

After linearisation of the additional energy arising from frictionless contact in the governing equation, the finite element discretisation of the fully coupled equations can be expressed as presented in [59, 62]:

$$\mathbf{M_u}\ddot{\mathbf{U}} + \mathbf{C}\dot{\mathbf{U}} + \int \mathbf{B}^T \boldsymbol{\sigma} d\Omega + \bigcup_{i=1}^{n_s} \mathbf{K}_{NC_i} = \mathbf{F_u} + \bigcup_{i=1}^{n_s} \mathbf{F}_{NC_i} \tag{87}$$

$$\mathbf{M_w}\ddot{\mathbf{U}} + \mathbf{Q}_\mathbf{w}^T\dot{\mathbf{U}} + \mathbf{C_{ww}}\dot{\mathbf{P}}_\mathbf{w} + \mathbf{C_{wc}}\dot{\mathbf{P}}_\mathbf{c} + \mathbf{H_{ww}}\mathbf{P_w} + \mathbf{H_{wc}}\mathbf{P_c} = \mathbf{F_w} \tag{88}$$

$$\mathbf{M_c}\ddot{\mathbf{U}} + \mathbf{R}_\mathbf{c}^T\dot{\mathbf{U}} + \mathbf{C_{cw}}\dot{\mathbf{P}}_\mathbf{w} + \mathbf{C_{cc}}\dot{\mathbf{P}}_\mathbf{c} + \mathbf{H}_\mathbf{wc}^T\mathbf{P_w} + \mathbf{H_{cc}}\mathbf{P_c} = \mathbf{F_c} \tag{89}$$

where n_s is the number of active contact segments. The unknown variables in the equations are displacement, pore water pressure, and suction represented by $\mathbf{U}$, $\mathbf{P_w}$ and $\mathbf{P_c}$, respectively. The force vectors and matrices (Appendix A) are denoted by F, M, Q, H, and C. The subscripts NC, u, w, and c denote the association of a force vector or matrix to normal contact and the degrees of freedom of displacement, pore water pressure, and suction. The definitions of all matrices as well as the contacted-related terms, $\mathbf{K}_{NC_i}$ and $\mathbf{F}_{NC_i}$, are given in [62].

The load and the flow vectors appearing in the governing finite element equations are defined by:

$$\mathbf{F_u} = \int_\Omega \mathbf{N_u^T} \rho \mathbf{b} d\Omega + \int_{\Gamma_t} \mathbf{N_u^T} \bar{\mathbf{t}} d\Gamma \tag{90}$$

$$\mathbf{F_w} = \int_\Omega \left(\text{grad}(\mathbf{N_{pw}})\right)^T \left(\mathbf{k}_g \rho_g + \mathbf{k}_w \rho_w\right) \mathbf{b} d\Omega$$
$$- \int_{\Gamma_{qw}} \mathbf{N_{pw}^T} \overline{w}_w d\Gamma - \int_{\Gamma_{qw} \cap \Gamma_{qg}} \mathbf{N_{pw}^T} \overline{w}_g d\Gamma$$
$$- \int_{\Gamma_{Pc} \cap \Gamma_{qw}} \mathbf{N_{pw}^T} \dot{\mathbf{w}}_g^T \mathbf{n}^* d\Gamma$$
$$- \int_\Omega \mathbf{N_{pw}^T} \left(\frac{\dot{\mathbf{w}}_w^T}{\rho_w}.\text{grad}(\rho_w) + \frac{\dot{\mathbf{w}}_g^T}{\rho_g}.\text{grad}(\rho_g)\right) d\Omega \tag{91}$$

$$\mathbf{F_c} = \int_\Omega \left(\text{grad}(\mathbf{N_{pc}})\right)^T \mathbf{k}_g \rho_g \mathbf{b} \, d\Omega - \int_{\Gamma_{qg}} \mathbf{N_{pc}^T} \overline{w}_g \, d\Gamma$$
$$- \int_\Omega \mathbf{N_{pc}^T} \frac{\dot{\mathbf{w}}_g^T}{\rho_g}.\text{grad}(\rho_g) \, d\Omega \tag{92}$$

The convective terms $\text{grad}(\rho_\beta)$ that appears in Eqs. (91) and (92) is sometimes assumed to be negligible (e.g., [61, 63]). Nonetheless, if the incorporation of such a term is needed in the analysis, such a term can be converted to $\text{grad}(p_\beta)$ using Eq. (13) or more sophisticated alternatives (see [38]).

Linearisation of the term $\int \mathbf{B}^T \sigma d\Omega$ depends on the choice of work-conjugate pairs used to develop the constitutive model as discussed in Sect. 2.3.1. For instance, if the approach outlined in Eq. (72) is adopted, in an elastoplastic analysis, Eq. (87) may be written as follows:

$$\mathbf{M_u}\ddot{\mathbf{U}} + \mathbf{C}\dot{\mathbf{U}} + \mathbf{K}\mathbf{U} + \bigcup_{i=1}^{n_s} \mathbf{K}_{NC_i} - \mathbf{Q_w}\mathbf{P_w} - \mathbf{Q_c^*}\mathbf{P_c}$$
$$= \mathbf{F_u} + \bigcup_{i=1}^{n_s} \mathbf{F}_{NC_i} \tag{93}$$

where since the degree of saturation is a function of suction and strain, we can assume:

$$d\boldsymbol{\sigma}' = \overline{\overline{\mathbf{D}}} : d\boldsymbol{\varepsilon} + \overline{\overline{\mathbf{S}}} dp_c \tag{94}$$

By assuming $\mathbf{m}^T = \left\{1\,1\,1\,0\,0\,0\right\}$, $\overline{\overline{\mathbf{D}}}$ and $\overline{\overline{\mathbf{S}}}$ will be obtained as follows:

$$\overline{\overline{\mathbf{D}}} = \mathbf{D}_{\boldsymbol{\sigma\sigma}} + \frac{\partial S_w}{\partial \varepsilon_v} \mathbf{D}_{\boldsymbol{\sigma}\overline{p}_c} \otimes \mathbf{m} \tag{95}$$

and

$$\overline{\overline{\mathbf{S}}} = \frac{\partial S_w}{\partial p_c} \mathbf{D}_{\boldsymbol{\sigma}\overline{p}_c} \tag{96}$$

Therefore, according to Eq. (41), $\mathbf{K}$ or the so-called stiffness matrix depends on both $\mathbf{D}_{\boldsymbol{\sigma\sigma}}$ and $\mathbf{D}_{\boldsymbol{\sigma}\overline{p}_c}$. Additionally,

$$\mathbf{Q_c^*} = \mathbf{Q_c} + \mathbf{Q_c^2} \text{ where } \mathbf{Q_c} = \int_\Omega \mathbf{B}^T \left(1 - S_w^{\left(\frac{\beta_1}{s_w^{\beta_2}}\right)}\right) \mathbf{m} \mathbf{N_{pc}} d\Omega$$

and $\mathbf{Q_c^2}$ results from the contribution of $\mathbf{D}_{\boldsymbol{\sigma}\overline{p}_c}$ in the model and may be defined as follows:

$$\mathbf{Q_c^*} = \int_\Omega \mathbf{B}^T \overline{\overline{\mathbf{S}}} \mathbf{N_{pc}} d\Omega \tag{97}$$

Time integration is done following the extension of the generalised-α method to fully coupled analysis in [64]. Also, a special case of this approach known as the Newmark method is presented in [60].

If hydraulic hysteresis is ignored, the equation SWRC can be obtained following the suggestion in [65] by defining a scaled suction, $p_c^* = p_c e^{\Omega'}$ (where e is the void ratio and Ω' is a material parameter regulating the impact of void ratio on SWRC) as follows [40]:

$$S_w^d = \left(1 + \left(P^d p_c^*\right)^{n_v^d}\right)^{-m_v^d} \tag{98}$$

where P^d denotes the inverse of the air-entry value. n_v^d and m_v^d are the model parameters that control the slope of the SWRC. In the presence of hysteresis, it is assumed that the main wetting and drying curves can be described by Eq. (98). The region bounded by the two curves is described by 'scanning curves' through an incremental relationship between the changes of the saturation degree as follows [40]:

$$dS_w = Y^*.dp_c^* \tag{99}$$

with Y^* defined as follows

$$Y^* = \left(\frac{p_c^*}{p_c^{*\alpha}}\right)^{b_\alpha} \frac{\partial S_w^\alpha}{\partial p_c^*} + Y^{*sc} \, (\alpha = w, d) \tag{100}$$

where w and d denote wetting and drying, respectively, and $p_c^{*\alpha}$ is defined by:

$$p_c^{*\alpha} = S_w^{\alpha-1}(S_w), \, (\alpha = w, d) \tag{101}$$

Also, b_w and b_d are model constants with negative and positive quantities in the wetting and drying processes, respectively. Moreover, in Eq. (100), Y^{*sc} ensures smooth

transitions between the wetting and drying curves on the scanning curves and is defined as follows:

$$Y^{*sc} = Y^{*r} \left(\frac{p_c^* - p_c^{*\alpha}}{p_c^{*r} - p_c^{*\alpha}} \right)^{b_{sc}}, \ (\alpha = w, d) \qquad (102)$$

where Y^{*r} is the slope of the scanning curve that will be stored in the memory upon a reversal in the wetting/drying process [40]. b_{sc} can be considered 25 as a default. Other parameters in the upcoming analyses are set as follows: $P^d = \frac{P^w}{2} = 98 \ kPa^{-1}$, $n_v^d = n_v^w = 0.28$, $m_v^d = m_v^w = 0.98$, and $b_d = -b_w = 3.0$, and $\Omega' = 10.6$.

In the coming examples, we compare two cases with different values of β_1 and β_2 in the effective stress equation. We assess the ground using a contact-impact model that transmits an impulse load with a duration of 0.3 and a peak of 1.0 kN. In all analyses, we convert the measured displacement at the centre of the impact to a dynamic hardness or indentation hardness, K_d which is defined as the peak impact force, F_{max} divided by the peak of displacement, u_{max} as follows:

$$K_d = \frac{F_{max}}{u_{max}} \qquad (103)$$

In the mechanical model, we use the non-linear elastic model for unsaturated soils presented in [66] as follows:

$$K = K_0 p_{atm} \frac{1+e}{e} \left(\frac{p\prime}{p_{atm}} \right)^{\frac{2}{3}} \qquad (104)$$

where p_{atm} is the atmospheric pressure, $p\prime$ represents the mean effective stress, and K_0 is a material parameter that is assumed to be 150 in all the coming analyses.

The shear modulus, G, is defined by:

$$G = G_0 p_{atm} \frac{(2.97 - e)^2}{1 + e} \left(\frac{p\prime}{p_{atm}} \right)^{\frac{1}{2}} \qquad (105)$$

where G_0 is a material parameter that is set to 125 in the simulations. It should be noted that a minimum pressure of 0.1 kPa is chosen in all the analyses for $p\prime$ to avoid numerical instability when the initial mean effective stress is close to zero (e.g., near saturation). A 2 m by 2 m domain of unsaturated soil (which is schematically shown in Fig. 5) is discretised into 900 nodes and 410 6-noded quadratic elements for displacement coupled with two 3-noded elements for pore water pressure and suction. The side boundaries of the mesh are restrained against horizontal displacements, and vertical displacements are not allowed at the bottom boundary. Drainage occurs only from the top boundary portion that is not in contact with the impervious plate. The initial void ratio is 0.5, and the hydraulic state of the material is assumed to be lying on the main drying curve. The at-rest earth pressure coefficient
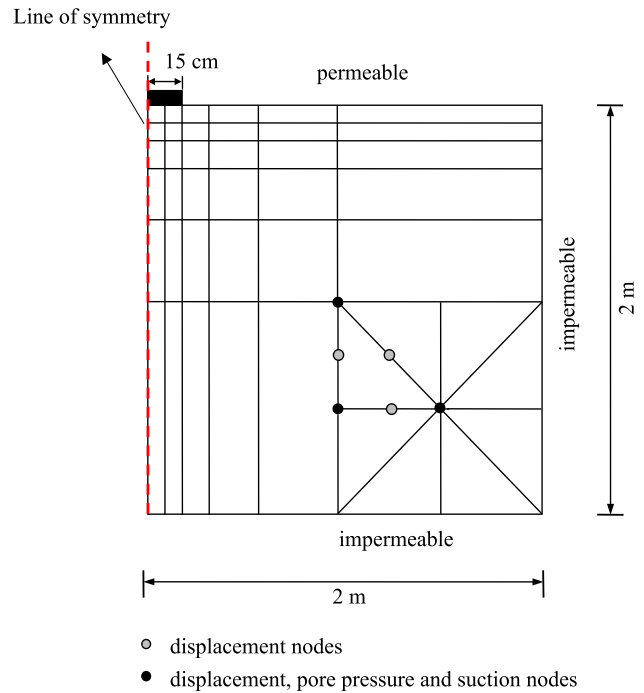

Fig. 5 Schematic representation of the Finite Element model

Table 1 The constitutive and general material parameters

Description	Symbol	Value	Unit
Density of solid particles	ρ_s	2700	Kg m^{-3}
Density of water	ρ_w	997	Kg m^{-3}
Density of air	ρ_a	1.1	Kg m^{-3}
Bulk modulus of water	K_w	2.25×10^6	kPa
Bulk modulus of air	K_g	1.01×10^2	kPa
Intrinsic permeability in the saturated state	k	1×10^{-10}	m^2
Viscosity of water	η_w	1.0×10^{-3}	Ns m^{-2}
Viscosity of air	η_a	1.8×10^{-5}	Ns m^{-2}

is 0.4, and geostatic stress is established initially. Dynamic plate-soil interaction is simulated using 1000 time steps of size 0.00003 s. Other parameters of the analysis are given in Table 1.

Figure 6a displays the selected forms for χ used in the analyses, and Fig. 6b and c show the corresponding shapes of χp_c. When $\chi = S_w^{\left(\frac{\beta_1}{S_w \beta_2} \right)}$, the pair of the effective stress parameters [β_1, β_2] are assigned the following values of [2.0, 0.5] (the reference case), [2.0, 0.4], and [1.5, 0.5]. It can be
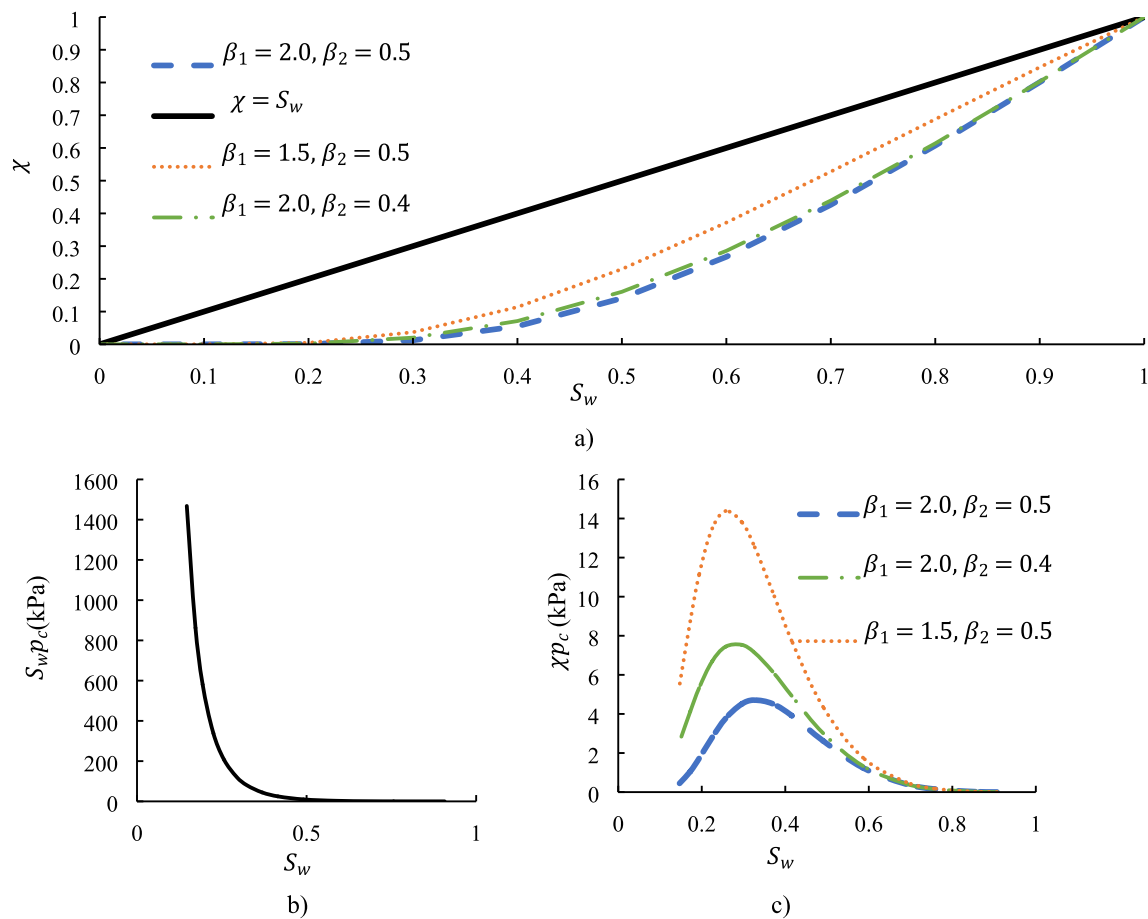
Fig. 6 **a** Assumed forms for χ in the analyses. **b** $S_w p_c$. c) $S_w^{\left(\frac{\beta_1}{S_w^{\beta_2}}\right)} p_c$

observed that, for the selected SWRC parameter, the term $S_w p_c$ increases continuously as the material becomes drier, whereas the presented effective stress model predicts a peak for χp_c at a degree of saturation of approximately 0.3 in the reference case. The two other cases with the proposed effective stress illustrate the impact of β_1 and β_2 on the predictions relative to the reference case. When β_1 is decreased at a given β_2, the effect of capillary suction decreases at a slower rate, and consequently, the peak in the χp_c term shifts towards dryness and increases in magnitude. Similarly, when β_2 is decreased at a given β_1, the peak also shifts towards dryness and increases.

The predicted dynamic hardness during the contact in both series of analyses is shown in Fig. 7. The dynamic hardness is investigated at 15 different initial suction values ranging from 0.005 to 10,000 kPa (0.005, 0.03, 0.3, 1, 5, 20, 60, 120, 250, 400, 800, 1500, 3000, 5000, and 10,000 kPa). Figure 7.a reveals that an ever-increasing dynamic hardness is predicted as the material becomes drier when the degree of saturation is selected as χ. However, the proposed effective stress model can only predict an increase in dynamic hardness up to a

degree of saturation of roughly 0.3 for the reference case, as shown in Fig. 7b. Below this degree of saturation, the dynamic hardness decreases. The other two cases, also indicate that decreasing β_1 and β_2 results in an increase in the predicted dynamic hardness. Moreover, the peak of the hardness shifts towards dryness as these values decrease.

The reason for the difference in the predicted dynamic hardness between the two approaches is due to the way they modify the initial mean effective stress and consequently, the elastic modulus per Eqs. (104) and (105). In the first approach, the effective mean stress is allowed to increase indefinitely, leading to a continuous increase in the predicted dynamic hardness. On the other hand, the proposed effective stress model restricts the increase in effective mean stress to a certain degree of saturation, beyond which it assumes a more prominent vanishing capillary effect and a decline in effective stress. As a result, the increase in dynamic hardness is controlled and limited, leading to a different prediction of dynamic hardness as compared to the first approach.
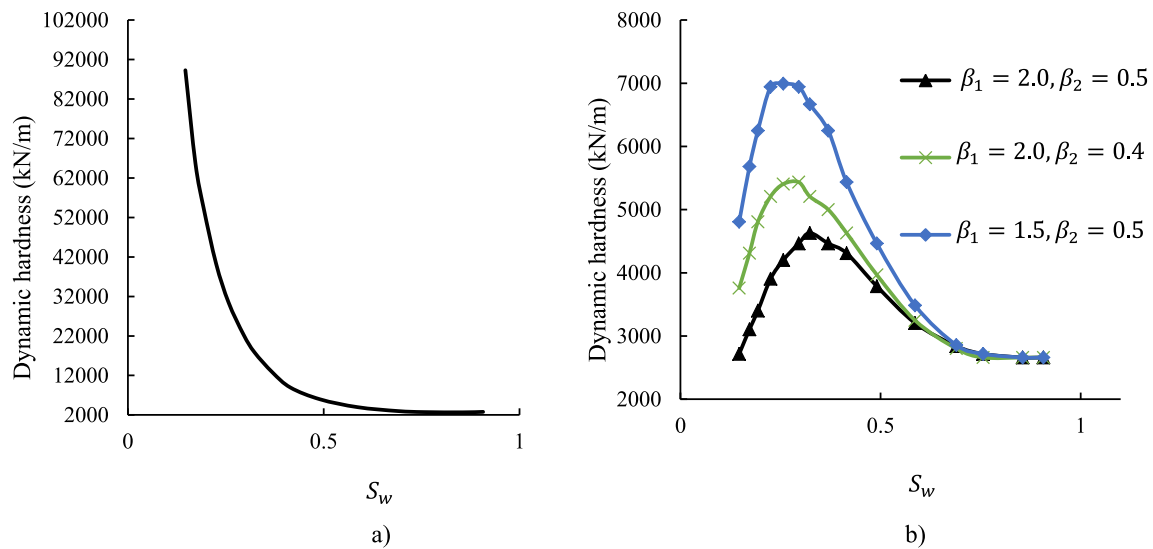
Fig. 7 Obtained dynamic hardness when **a** $\chi = S_w$. **b** $\chi = S_w^{\left(\frac{\beta_1}{S_w^{\beta_2}}\right)}$

4 Conclusion

This paper presented an extension of Biot's theory of dynamic wave propagation in fluid-saturated media to model dynamic structural interactions with soils across a wide range of degrees of saturation. This was achieved by introducing a novel definition for effective stress, which is founded on a rigorous thermodynamic basis and validated against experimental evidence. Additionally, work-conjugate pairs for the new effective stress are identified. The capabilities of a fully coupled finite element contact model based on the new effective stress parameters are then demonstrated through numerical examples. Results indicate that the new model successfully allows controlling the vanishing effect of capillary suction toward dryness.

Appendix A

The finite element matrices and vectors are defined by:

$$\mathbf{M_u} = \int_\Omega \mathbf{N_u}^T \rho \mathbf{N_u} d\Omega \tag{106}$$

$$\mathbf{M_w} = \int_\Omega \left(\mathrm{grad}(\mathbf{N_{pw}})\right)^T \left(\mathbf{k}_g \rho_g + \mathbf{k}_w \rho_w\right)\mathbf{N_u} d\Omega \tag{107}$$

$$\mathbf{Q_w} = \int_\Omega \mathbf{B}^T \mathbf{m}\mathbf{N_{pw}} d\Omega \tag{108}$$

$$\mathbf{M_C} = \int_\Omega \left(\mathrm{grad}(\mathbf{N_{pc}})\right)^T \mathbf{k}_g \rho_g \mathbf{N_u} d\Omega \tag{109}$$

$$\mathbf{H_{ww}} = \int_\Omega \left(\mathrm{grad}(\mathbf{N_{pw}})\right)^T \left(\mathbf{k}_g + \mathbf{k}_w\right)\left(\mathrm{grad}(\mathbf{N_{pw}})\right)d\Omega \tag{110}$$

$$\mathbf{H_{cc}} = \int_\Omega \left(\mathrm{grad}(\mathbf{N_{pc}})\right)^T \left(\mathbf{k}_g\right)\left(\mathrm{grad}(\mathbf{N_{pc}})\right)d\Omega \tag{111}$$

$$\mathbf{H_{wc}} = \int_\Omega \left(\mathrm{grad}(\mathbf{N_{pw}})\right)^T \left(\mathbf{k}_g\right)\left(\mathrm{grad}(\mathbf{N_{pc}})\right)d\Omega \tag{112}$$

$$\mathbf{C_{ww}} = \int_\Omega \mathbf{N_{pw}}^T C_1^* \mathbf{N_{pw}} d\Omega \tag{113}$$

$$\mathbf{C_{cc}} = \int_\Omega \mathbf{N}_{\mathbf{pc}}^T C_2^* \mathbf{N_{pc}} d\Omega \tag{114}$$

$$\mathbf{C_{wc}} = \int_\Omega \mathbf{N}_{\mathbf{pw}}^T C_3^* \mathbf{N_{pc}} \, d\Omega \tag{115}$$

$$\mathbf{C_{cw}} = \int_\Omega \mathbf{N}_{\mathbf{pc}}^T C_3^* \mathbf{N_{pw}} d\Omega \tag{116}$$

$$\mathbf{R_c} = \int_\Omega \mathbf{B}^T C_6 \mathbf{m} \mathbf{N_{pc}} d\Omega \tag{117}$$

Also, we define.

$$C_1^* = \frac{nS_w}{K_w} + \frac{nS_g}{K_g} \tag{118}$$

$$C_2^* = S_g \frac{n}{K_g} - n \frac{\partial S_w}{\partial p_c} \tag{119}$$

$$C_3^* = S_g \frac{n}{K_g} \tag{120}$$

$$C_6 = 1 - \left(S_w + e \frac{\partial S_w}{\partial e} \right) \tag{121}$$

References

1. Biot MA (1956) Theory of propagation of elastic waves in a fluid-saturated porous solid. II. Higher frequency range. J Acoust Soc Am 28(2):179–191
2. Biot MA (1956) Theory of propagation of elastic waves in a fluid-saturated porous solid. I. Low-frequency range. J Acoust Soc Am 28(2):168
3. Zienkiewicz OC, Chan A, Pastor M, Paul D, Shiomi T (1990) Static and dynamic behaviour of soils: a rational approach to quantitative solutions. I. Fully saturated problems. Proc R Soc Lond A Math Phys Sci 429(1877):285–309
4. Schanz M (2009) Poroelastodynamics: linear models, analytical solutions, and numerical methods. Appl Mech Rev 62(3):030803
5. Jassim I, Stolle D, Vermeer P (2013) Two-phase dynamic analysis by material point method. Int J Numer Anal Meth Geomech 37(15):2502–2522
6. Pastor M, Yague A, Stickle M, Manzanal D, Mira P (2018) A two-phase SPH model for debris flow propagation. Int J Numer Anal Meth Geomech 42(3):418–448
7. Zienkiewicz OC, Xie Y, Schrefler B, Ledesma A, Biĉaniĉ N (1990) Static and dynamic behaviour of soils: a rational approach to quantitative solutions. II. Semi-saturated problems. Proc R Soc Lond A Math Phys Sci 429(1877):311–321
8. Li X, Zienkiewicz O (1992) Multiphase flow in deforming porous media and finite element solutions. Comput Struct 45(2):211–227
9. Bishop AW, Blight G (1963) Some aspects of effective stress in saturated and partly saturated soils. Geotechnique 13(3):177–197
10. Schrefler BA (1984) The finite element method in soil consolidation: (with applications to surface subsidence), PhD, University College of Swansea
11. Houlsby G (1997) The work input to an unsaturated granular material. Géotechnique 47(1):193–196
12. Borja RI (2004) Cam-clay plasticity. Part V: a mathematical framework for three-phase deformation and strain localization analyses of partially saturated porous media. Comput Methods Appl Mech Eng 193(48):5301–5338. https://doi.org/10.1016/j.cma.2003.12.067
13. Schrefler B (2002) Mechanics and thermodynamics of saturated/unsaturated porous materials and quantitative solutions. Appl Mech Rev 55(4):351–388
14. Lu N, Godt JW, Wu DT (2010) A closed—form equation for effective stress in unsaturated soil. Water Resour Res 46(5)
15. Konrad J-M, Lebeau M (2015) Capillary-based effective stress formulation for predicting shear strength of unsaturated soils. Can Geotech J 52(12):2067–2076
16. Alonso EE, Pereira J-M, Vaunat J, Olivella S (2010) A microstructurally based effective stress for unsaturated soils. Géotechnique 60(12):913–925
17. Alonso EE, Pinyol N, Gens A (2013) Compacted soil behaviour: initial state, structure and constitutive modelling. Géotechnique 63(6):463–478
18. Khalili N, Zargarbashi S (2010) Influence of hydraulic hysteresis on effective stress in unsaturated soils. Géotechnique 60(9):729–734
19. Chen K, He X, Liang F, Sheng D (2023) Contribution of capillary pressure to effective stress for unsaturated soils: role of wet area fraction and water retention curve. Comput Geotech 154:105140
20. Lewis R, Schrefler B (1999) The finite element method in the static and dynamic deformation and consolidation of porous media. Meccanica 34(3):231–232
21. Karube D, Kato S (1989) Yield functions of unsaturated soil. In: Congrès international de mécanique des sols et des travaux de fondations, vol 12, pp 615–618
22. Karube D, Kato S (1994) An ideal unsaturated soil and the Bishop's soil. In: International conference on soil mechanics and foundation engineering, pp 43–46.
23. Karube D, Kato S, Hamada K, Honda M (1996) The relationship between the mechanical behavior and the state of porewater in unsaturated soil. Doboku Gakkai Ronbunshu 1996(535):83–92
24. Lu N, Likos WJ (2006) Suction stress characteristic curve for unsaturated soil. J Geotech Geoenviron Eng 132(2):131–142
25. Kim B, Shibuya S, Park S, Kato S (2013) Suction stress and its application on unsaturated direct shear test under constant volume condition. Eng Geol 155:10–18
26. Khalili N, Khabbaz M (1998) A unique relationship for χ for the determination of the shear strength of unsaturated soils. Geotechnique 48(5):681–687
27. Sheng D, Sloan SW, Gens A, Smith DW (2003) Finite element formulation and algorithms for unsaturated soils. Part I: Theory. Int J Numer Anal Meth Geomech 27(9):745–765
28. Verdugo R, Ishihara K (1996) The steady state of sandy soils. Soils Found 36(2):81–91
29. Gallipoli D, Gens A, Sharma R, Vaunat J (2003) An elasto-plastic model for unsaturated soil incorporating the effects of suction and degree of saturation on mechanical behaviour. Géotechnique 53(1):123–136
30. Wheeler S, Sharma R, Buisson M (2003) Coupling of hydraulic hysteresis and stress–strain behaviour in unsaturated soils. Géotechnique 53(1):41–54
31. Airey DW, Ghorbani J (2021) Analysis of unsaturated soil columns with application to bulk cargo liquefaction in ships. Comput Geotech 140:104402
32. Khalili N, Geiser F, Blight G (2004) Effective stress in unsaturated soils: Review with new evidence. Int J Geomech 4(2):115–126
33. Fredlund DG, Morgenstern NR (1977) Stress state variables for unsaturated soils. J Geotech Eng Div 103(5):447–466

34. Hassanizadeh M, Gray WG (1979) General conservation equations for multi-phase systems: 1. Averaging procedure. Adv Water Resour 2:131–144

35. Brooks R, Corey A (1964) Hydraulic properties of porous media and their relation to drainage design. Trans ASAE 7(1):26–0028

36. Van Genuchten MT (1980) A closed-form equation for predicting the hydraulic conductivity of unsaturated soils. Soil Sci Soc Am J 44(5):892–898

37. Borja RI (2006) On the mechanical energy and effective stress in saturated and unsaturated porous continua. Int J Solids Struct 43(6):1764–1786

38. Zhao Y, Borja RI (2020) A continuum framework for coupled solid deformation–fluid flow through anisotropic elastoplastic porous media. Comput Methods Appl Mech Eng 369:113225

39. Ghorbani J, Airey DW (2019) Some aspects of numerical modelling of hydraulic hysteresis of unsaturated soils. In: Hertz M (ed) Unsaturated soils: behavior, mechanics and conditions. Nova Science Publishers

40. Ghorbani J, Airey DW, El-Zein A (2018) Numerical framework for considering the dependency of SWCCs on volume changes and their hysteretic responses in modelling elasto-plastic response of unsaturated soils. Comput Methods Appl Mech Eng 336:80–110

41. Khalili N, Habte M, Zargarbashi S (2008) A fully coupled flow deformation model for cyclic analysis of unsaturated soils including hydraulic and mechanical hystereses. Comput Geotech 35(6):872–889

42. Einav I, Liu M (2023) Hydrodynamics of non—equilibrium soil water retention. Water Resour Res 59(1):e2022WR033409

43. Zhou A-N, Sheng D, Sloan SW, Gens A (2012) Interpretation of unsaturated soil behaviour in the stress–saturation space, I: volume change and water retention behaviour. Comput Geotech 43:178–187

44. Uzuoka R, Borja RI (2012) Dynamics of unsaturated poroelastic solids at finite strain. Int J Numer Anal Meth Geomech 36(13):1535–1573. https://doi.org/10.1002/nag.1061

45. Khoei A, Saeedmonir S (2021) Computational homogenization of fully coupled multiphase flow in deformable porous media. Comput Methods Appl Mech Eng 376:113660

46. Chen L, Ghorbani J, Zhang C, Dutta TT, Kodikara J (2021) A novel unified model for volumetric hardening and water retention in unsaturated soils. Comput Geotech 140:104446

47. Ghorbani J, Airey DW, Carter JP, Nazem M (2021) Unsaturated soil dynamics: finite element solution including stress-induced anisotropy. Comput Geotech 133:104062. https://doi.org/10.1016/j.compgeo.2021.104062

48. Santagiuliana R, Schrefler BA (2006) Enhancing the Bolzon–Schrefler–Zienkiewicz constitutive model for partially saturated soil. Transp Porous Media 65(1):1–30. https://doi.org/10.1007/s11242-005-6083-6

49. Sheng D, Sloan S, Gens A (2004) A constitutive model for unsaturated soils: thermomechanical and computational aspects. Comput Mech 33:453–465

50. Phan DG, Nguyen GD, Bui HH, Bennett T (2021) Constitutive modelling of partially saturated soils: hydro-mechanical coupling in a generic thermodynamics-based formulation. Int J Plast 136:102821

51. Buscarnera G, Nova R (2011) Modelling instabilities in triaxial testing on unsaturated soil specimens. Int J Numer Anal Meth Geomech 35(2):179–200

52. Kodikara J, Jayasundara C, Zhou A (2020) A generalised constitutive model for unsaturated compacted soils considering wetting/drying cycles and environmentally-stabilised line. Comput Geotech 118:103332

53. Pestana JM, Whittle AJ (1999) Formulation of a unified constitutive model for clays and sands. Int J Numer Anal Meth Geomech 23(12):1215–1243

54. Borja RI, Tamagnini C (1998) Cam-clay plasticity Part III: extension of the infinitesimal model to include finite strains. Comput Methods Appl Mech Eng 155(1–2):73–95

55. Zytynski M, Randolph M, Nova R, Wroth C (1978) On modelling the unloading-reloading behaviour of soils. Int J Numer Anal Meth Geomech 2(1):87–93

56. Song X, Borja RI (2014) Mathematical framework for unsaturated flow in the finite deformation range. Int J Numer Meth Eng 97(9):658–682

57. Mašín D (2010) Predicting the dependency of a degree of saturation on void ratio and suction using effective stress principle for unsaturated soils. Int J Numer Anal Meth Geomech 34(1):73–90

58. Zhou A-N, Sheng D, Sloan SW, Gens A (2012) Interpretation of unsaturated soil behaviour in the stress–saturation space: II: constitutive relationships and validations. Comput Geotech 43:111–123

59. Ghorbani J, Chen L, Kodikara J, Carter JP, McCartney JS (2023) Memory repositioning in soil plasticity models used in contact problems. Comput Mech 71(3):385–408. https://doi.org/10.1007/s00466-022-02245-z

60. Khoei A, Mohammadnejad T (2011) Numerical modeling of multiphase fluid flow in deforming porous media: a comparison between two-and three-phase models for seismic analysis of earth and rockfill dams. Comput Geotech 38(2):142–166

61. Schrefler BA, Scotta R (2001) A fully coupled dynamic model for two-phase fluid flow in deformable porous media. Comput Methods Appl Mech Eng 190(24):3223–3246

62. Ghorbani J, Nazem M, Kodikara J, Wriggers P (2021) Finite element solution for static and dynamic interactions of cylindrical rigid objects and unsaturated granular soils. Comput Methods Appl Mech Eng 384:113974

63. Lewis RW, Schrefler BA (1998) The finite element method in the static and dynamic deformation and consolidation of porous media. Wiley

64. Ghorbani J, Nazem M, Carter J (2016) Numerical modelling of multiphase flow in unsaturated deforming porous media. Comput Geotech 71:195–206

65. Gallipoli D, Wheeler S, Karstunen M (2003) Modelling the variation of degree of saturation in a deformable unsaturated soil. Géotechnique 53(1):105–112

66. Ghorbani J, Airey DW (2021) Modelling stress-induced anisotropy in multi-phase granular soils. Comput Mech 67:497–521. https://doi.org/10.1007/s00466-020-01945-8. (**In Press**)